Two Distinct Aerobic Methionine Salvage Pathways Generate Volatile Methanethiol in *Rhodopseudomonas palustris*

Anthony R. Miller,[a] Justin A. North,[a] John A. Wildenthal,[a] F. Robert Tabita[a]

[a]Department of Microbiology, The Ohio State University, Columbus, Ohio, USA

ABSTRACT 5'-Methyl-thioadenosine (MTA) is a dead-end, sulfur-containing metabolite and cellular inhibitor that arises from *S*-adenosyl-L-methionine-dependent reactions. Recent studies have indicated that there are diverse bacterial methionine salvage pathways (MSPs) for MTA detoxification and sulfur salvage. Here, via a combination of gene deletions and directed metabolite detection studies, we report that under aerobic conditions the facultatively anaerobic bacterium *Rhodopseudomonas palustris* employs both an MTA-isoprenoid shunt identical to that previously described in *Rhodospirillum rubrum* and a second novel MSP, both of which generate a methanethiol intermediate. The additional *R. palustris* aerobic MSP, a dihydroxyacetone phosphate (DHAP)-methanethiol shunt, initially converts MTA to 2-(methylthio) ethanol and DHAP. This is identical to the initial steps of the recently reported anaerobic ethylene-forming MSP, the DHAP-ethylene shunt. The aerobic DHAP-methanethiol shunt then further metabolizes 2-(methylthio)ethanol to methanethiol, which can be directly utilized by O-acetyl-L-homoserine sulfhydrylase to regenerate methionine. This is in contrast to the anaerobic DHAP-ethylene shunt, which metabolizes 2-(methylthio)ethanol to ethylene and an unknown organo-sulfur intermediate, revealing functional diversity in MSPs utilizing a 2-(methylthio)ethanol intermediate. When MTA was fed to aerobically growing cells, the rate of volatile methanethiol release was constant irrespective of the presence of sulfate, suggesting a general housekeeping function for these MSPs up through the methanethiol production step. Methanethiol and dimethyl sulfide (DMS), two of the most important compounds of the global sulfur cycle, appear to arise not only from marine ecosystems but from terrestrial ones as well. These results reveal a possible route by which methanethiol might be biologically produced in soil and freshwater environments.

IMPORTANCE Biologically available sulfur is often limiting in the environment. Therefore, many organisms have developed methionine salvage pathways (MSPs) to recycle sulfur-containing by-products back into the amino acid methionine. The metabolically versatile bacterium *Rhodopseudomonas palustris* is unusual in that it possesses two RuBisCOs and two RuBisCO-like proteins. While RuBisCO primarily serves as the carbon fixation enzyme of the Calvin cycle, RuBisCOs and certain RuBisCO-like proteins have also been shown to function in methionine salvage. This work establishes that only one of the *R. palustris* RuBisCO-like proteins functions as part of an MSP. Moreover, in the presence of oxygen, to salvage sulfur, *R. palustris* employs two pathways, both of which result in production of volatile methanethiol, a key compound of the global sulfur cycle. When total available sulfur was plentiful, methanethiol was readily released into the environment. However, when sulfur became limiting, methanethiol release decreased, presumably due to methanethiol utilization to regenerate needed methionine.

KEYWORDS *Rhodopseudomonas palustris*, methanethiol, methionine salvage

In all cells, specific metabolic reactions are essential to maintain intracellular organic sulfur pools. For example, synthesis of sulfur-containing amino acids L-cysteine and L-methionine, coenzymes such as thiamine and coenzyme A, and cosubstrates such as glutathione and *S*-adenosyl-L-methionine (SAM) (Fig. 1; compound 2) requires sulfur in the proper oxidation state. In the environment, the total concentration of sulfur, usually in the form of sulfate, can be quite low, including in such environments as freshwater (~100 μM), anoxic bogs (~20 μM), and flooded soil ecosystems (20 μM to 20 mM) (1–5). Thus, in order to maintain proper intracellular organic sulfur levels, organisms have developed salvage pathways for recycling dead-end sulfur-containing by-products arising from key metabolic reactions. For example, nearly all organisms possess the active methyl cycle (6) to regenerate L-methionine from *S*-adenosyl-L-homocysteine, which is a by-product of SAM-dependent methyltransferase reactions. Similarly, SAM also serves as a cosubstrate for synthesis of polyamines (6), 1-aminocyclopropane-1-carboxylate (the ethylene precursor of plants) (7), acyl- and aryl-homoserine lactone quorum sensing compounds (8), phytosiderophores (9), and certain betaine lipids (10). As a result of these reactions, the inhibitory and dead-end by-product 5'-methyl-thioadenosine (MTA) is formed (Fig. 1; compound 3).

Intracellular buildup of MTA can result in cell cytotoxicity (6). Therefore, nearly all organisms, save some obligate endosymbionts/pathogens, possess either MTA/*S*-adenosylhomocysteine (SAH) nucleosidase (MtnN) (Fig. 1; enzyme B) or MTA phosphorylase (MtnP) (Fig. 1; enzyme D) for the hydrolysis or phosphorolysis of MTA to 5-(methylthio)ribose or 5-(methylthio)ribose-1-P (P, phosphate), respectively (6, 11). Organisms such as *Escherichia coli* that live in sulfur-rich environments simply excrete 5-(methylthio)ribose (Fig. 1; compound 4) into the environment at the expense of organic sulfur (12). However, given that many organisms encounter sulfur-limiting environments, further recycling of MTA to regenerate a usable sulfur source, typically L-methionine, is necessary to maintain proper cellular sulfur pools. This is underpinned by the fact that nearly all eukaryotes possess the universal methionine salvage pathway (MSP), also referred to as the canonical MSP or, in plant systems, the Yang cycle (Fig. 1; black). The canonical pathway consists of six enzymatic steps: nucleosidase/phosphory-lase (MtnP), isomerase (MtnA), dehydratase (MtnB), enolase/phosphatase (MtnC), di-oxygenase (MtnD), and transaminase (MtnE) (Fig. 1; enzymes D to F and enzymes I to K) (13). This results in the conversion of MTA to adenine, formate, and L-methionine at the expense of inorganic phosphate, molecular oxygen, and a suitable amino acid as an amine donor. Moreover, this process is inherently aerobic due to the oxygen require-ment of the dioxygenase.

While some bacteria also possess the canonical MSP, it is becoming increasingly evident that many bacteria have developed multiple variations of this pathway, some of which result in the production of novel metabolites, including isoprenoids and ethylene (14, 15). The *Bacillus* variation replaces the bifunctional enolase/phosphatase (MtnC concentration) (Fig. 1; enzyme I) with a RuBisCO-like protein (RLP), from the YkrW clade, functioning as a 2,3-diketo-5-methylthiopentyl-1-P enolase (MtnW) (Fig. 1; en-zyme G), and a separate 2-hydroxy-3-keto-5-methylthiopent(1)ene-1-P phosphatase (MtnX) (Fig. 1; enzyme H) (16, 17). Similarly, the *Tetrahymena* variation replaces MtnB, MtnC, and MtnD with a single multifunctional fusion enzyme (MtnBD) catalyzing the dehydratase, enolase, dioxygenase, and, possibly, phosphatase reactions (18). In these cases, the products and oxygen requirements are the same as those of the canonical MSP.

Alternatively, some proteobacteria contain genes encoding the MTA-isoprenoid shunt MSP, originally discovered in *Rhodospirillum rubrum* (Fig. 1; blue) (14), which results in the formation of 1-deoxyxylulose-5-P (DXP) for isoprenoid metabolism and of volatile methanethiol (Fig. 1; compound 13) for L-methionine regeneration (14). Unlike the canonical MSP, the MTA-isoprenoid shunt is oxygen independent and functions under both aerobic and anaerobic growth conditions in *R. rubrum* (14, 19). Analogous to the canonical MSP, the first two enzymatic steps of the MTA-isoprenoid shunt are catalyzed by MTA phosphorylase (MtnP) and 5-(methylthio)ribose-1-P isomerase (MtnA)
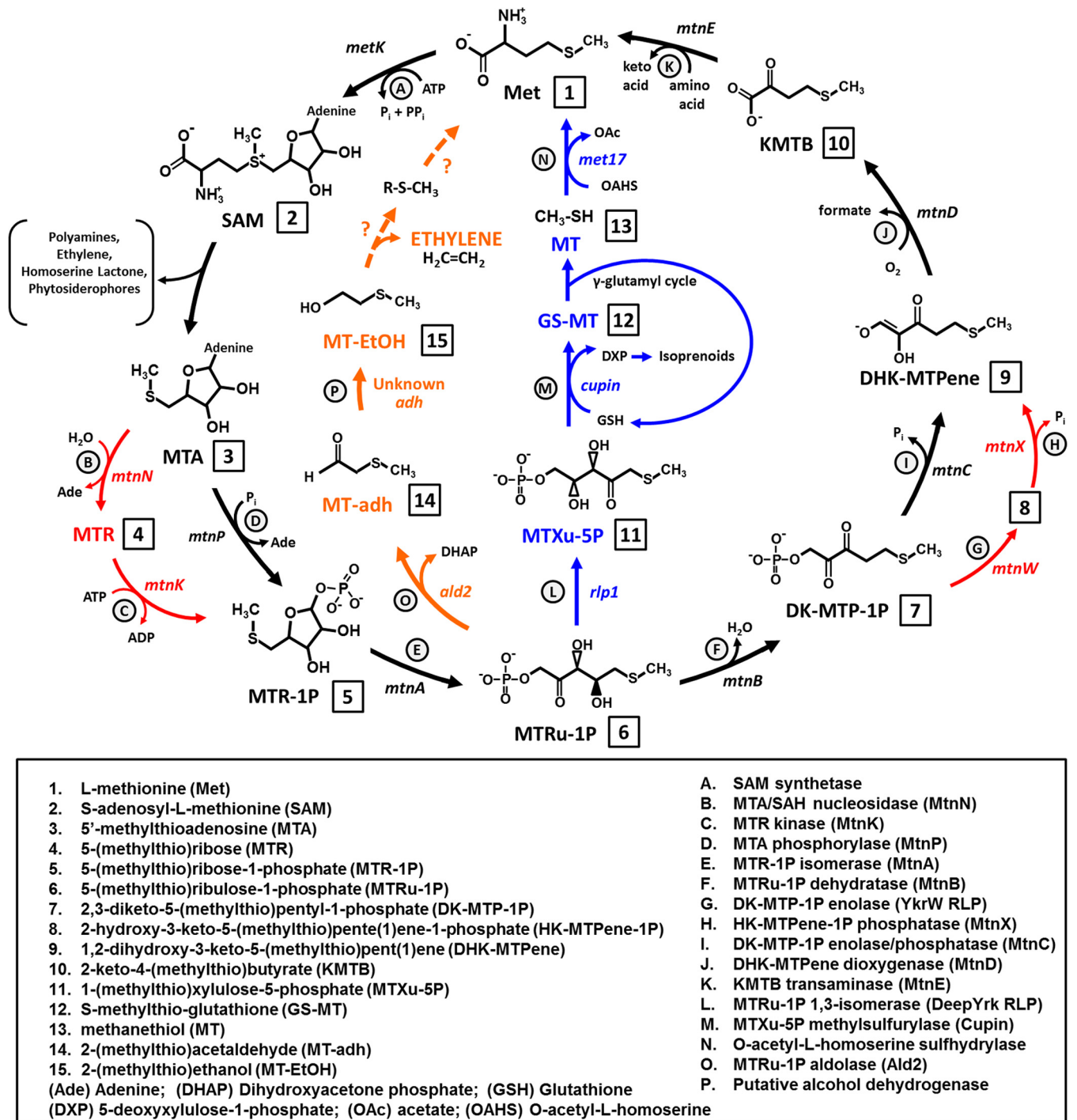
FIG 1 Previously identified bacterial variations on anaerobic and aerobic methionine salvage pathways (see reference 15). (Black) Strictly aerobic canonical ("universal") MSP from *Klebsiella pneumoniae*, also found in most eukaryotes (plants, animals, fungi). (Red) *Bacillus* sp. variation in which the MTA phosphorylase (MtnP) is replaced by an MTA nucleosidase (MtnN) and 5-(methylthio)ribose kinase (MtnK) and the bifunctional DK-MTP-1P enolase/phosphatase (MtnC) is replaced by a YkrW clade RLP (MtnW) functioning as a DK-MTP-1P enolase and a separate phosphatase (MtnX). (Blue) Aerobic-anaerobic MTA-isoprenoid shunt MSP in *R. rubrum* in which a DeepYkr clade RLP (Rlp1) functions as a 5-(methylthio)xylulose-1-P 1,3-isomerase to form 1-(methylthio)xylulose-5-P as a precursor to methanethiol and DXP for isoprenoid biosynthesis. (Orange) Exclusively anaerobic DHAP-ethylene shunt MSP from *R. rubrum* and *R. palustris* in which a novel class II aldolase (Ald2) catalyzes cleavage of 5-(methylthio)ribulose-1-P to form DHAP and 2-(methylthio)acetaldehyde as a precursor to ethylene. Compounds are indicated numerically; enzyme names are indicated alphabetically; gene designations are in italics.

(Fig. 1; enzymes D and E). Next, an RLP from the DeepYkr clade catalyzes the 1,3-isomerization of the resultant 5-(methylthio)ribulose-1-P to 1-(methylthio)xylulose-5-P and 1-(methylthio)ribulose-5-P at a 3:1 ratio (Fig. 1; enzyme L). Subsequently a cupin-type 1-(methylthio)xylulose-5-P methylsulfurylase catalyzes the glutathione-mediated

reduction of 1-(methylthio)xylulose-5-P to *S*-methylthio-glutathione and DXP (Fig. 1; enzyme M) (20, 21). During the process of glutathione regeneration, free methanethiol is proposed to be released either by the γ-glutamyl cycle, initiated by γ-glutamyl transferase (21), or by a putative specific methylthio-glutathione reductase (22). The liberated methanethiol couples to O-acetyl-L-homoserine (OAHS) catalyzed by the enzyme OAHS sulfhydrylase to regenerate L-methionine (Fig. 1; enzyme N) (14).

Further investigations into MTA metabolism in *R. palustris* and *R. rubrum* led to the discovery of an exclusively anaerobic ethylene-forming MSP (Fig. 1; orange) (15), which we formally name here the "DHAP-ethylene shunt" (for "dihydroxyacetone phosphate-methanethiol shunt") Like the canonical and MTA-isoprenoid shunt MSPs, the DHAP-ethylene shunt MSP proceeds via the activity of MtnP and MtnA (Fig. 1; enzymes D and E). However, the resultant 5-(methylthio)ribulose-1-P is then cleaved into dihydroxyacetone phosphate (DHAP) and 2-(methylthio)acetaldehyde by means of a class II aldolase-like protein (Ald2) functioning as a 5-(methylthio)ribulose-1P aldolase (Fig. 1; enzyme O). The 2-(methylthio)acetaldehyde is subsequently reduced by a putative alcohol dehydrogenase to 2-(methylthio)ethanol (Fig. 1; enzyme P), which is further metabolized by an unknown enzyme(s) to recycle the methylthio moiety, generating ethylene in the process.

Lastly, in *R. rubrum*, bona fide RuBisCO is also absolutely required to support anaerobic MTA metabolism. Complementation studies performed with mutant RuBisCO proteins indicate that RuBisCO may function differently from the typical ribulose-1,5-bisphosphate-dependent CO_2 fixation reaction and is required for MTA metabolism. Complementation studies show also that all extant forms of RuBisCO (forms I, II, and III) can perform this unknown function, and metabolomics studies suggest that the unknown function may be linked to the formation of *S*-methyl-3-mercaptopyruvate and *S*-methyl-L-cysteine (23).

R. palustris is unique in that it possesses homologues for two RLPs (encoded by the *rlp1* and *rlp2* genes) and two RuBisCOs, (form I, encoded by *cbbLS*, and form II, encoded by *cbbM*) (24). RLP1 of *R. palustris* is homologous to the DeepYkr RLP from the *R. rubrum* MTA-isoprenoid shunt (Fig. 1; enzyme L), and RLP2 is homologous to the *Chlorobaculum tepidum* Photo RLP, which in *C. tepidum* is involved in a stress response and sulfur oxidation (25). Moreover, *R. palustris* contains all the requisite gene homologues for the MTA-isoprenoid shunt (Fig. 1; blue) (19) and also possesses a functional DHAP-ethylene shunt MSP (Fig. 1; orange) (15). As such, *R. palustris* is poised for metabolic versatility in its ability to metabolize MTA in order to maintain proper intracellular sulfur pools. However, the aerobic mechanisms of methionine salvage in this organism and, by extension, the function of the two distinct RLPs and RuBisCOs in sulfur metabolism are largely unknown.

In this study, we showed, through a combination of gene deletions and directed metabolite detection studies, that under aerobic conditions, *R. palustris* contains both a functional MTA-isoprenoid shunt and an additional aerobic MSP, which we name the "DHAP-methanethiol shunt MSP." Analogous to the exclusively anaerobic DHAP-ethylene shunt from *R. rubrum* and *R. palustris* (Fig. 1; orange) (15), the *R. palustris* aerobic DHAP-methanethiol shunt initially proceeds by converting MTA to 2-(methylthio)ethanol and DHAP via MtnP, MtnA, Ald2, and a putative alcohol dehydrogenase (Fig. 1; enzymes D, E, O, and P). However, this novel *R. palustris* aerobic DHAP-methanethiol shunt MSP then employs an unknown enzyme(s) for methionine regeneration, resulting in metabolism of 2-(methylthio)ethanol into volatile methanethiol. This is in contrast to the results seen with the exclusively anaerobic DHAP-ethylene shunt MSP, which instead further metabolizes 2-(methylthio)ethanol via an unknown enzyme(s) into ethylene and an unknown organo-sulfur intermediate for methionine regeneration. Presumably, as with the *R. rubrum* MTA-isoprenoid shunt (Fig. 1; enzyme N) (14), the homologous *R. palustris* OAHS sulfhydrylase (Met17) regenerates methionine from the liberated methanethiol and O-acetyl-L-homoserine. Feeding experiments performed with ¹⁴C-labeled MTA indicated that the two pathways function simultaneously, suggesting a partitioning of MTA between DXP and DHAP

TABLE 1 *R. palustris* strains used in this study

| *R. palustris* strain	Growth phenotype or description[a]	Reference	Aerobic growth doubling time (h)[b]	
			SO_4^{-2}	MTA
Wild type	CGA010, St[r]	43	22 ± 3	20 ± 3
Δ*rlp1*	Rlp1; DeepYkr clade RLP (ΔRPA2169)	15	25 ± 3	27 ± 3
Δ*rlp2*	Rlp2⁻; Photo clade RLP (ΔRPA0262)	15	27 ± 1	26 ± 1
Δ*rlp12*	Δ*rlp1* Δ*rlp2*	This study	27 ± 2	28 ± 3
Δ*cupin*	Cupin⁻; MTXu-5P methylsulfurylase (ΔRPA2170)	15	22 ± 3	27 ± 5
Δ*quad*	Δ*rlp1* Δ*rlp2* RbcL⁻ (ΔRPA1559) CbbM⁻ (ΔRPA4041)	This study	19 ± 2	19 ± 3
Δ*quad* Δ*cupin*	Δ*rlp1* Δ*rlp2* Δ*rbcL* Δ*cbbM* Δcupin	This study	20 ± 3	22 ± 2
Δ*mtnP*	MtnP⁻; MTA phosphorylase (ΔRPA4821)	15	19 ± 2	NG
Δ*mtnP*::pBBR1	Δ*mtnP* complemented with pBBR1	15	19 ± 2	NG
Δ*mtnP*::pBBR1-RpMtnP	Δ*mtnP* complemented with pBBR1 bearing *mtnP*	15	20 ± 3	20 ± 2
Δ*mtnA*	ΔMTR-1P isomerase (RPA4820)	15	21 ± 2	NG
Δ*mtnA*::pBBR1	Δ*mtnA* complemented with pBBR1	15	25 ± 1	NG
Δ*mtnA*::pBBR1-RpMtnA	Δ*mtnA* complemented with pBBR1 bearing *mtnA*	15	23 ± 2	18 ± 2
Δ*ald2*	Ald2⁻; MTRu-1P aldolase (ΔRPA4655)	15	19 ± 3	21 ± 2
Δ*rlp1* Δ*ald2*	Δ*rlp1* Δ*ald2*	This study	20 ± 6	60 ± 3
Δ*rlp1* Δ*ald2*::pBBR1	Δ*rlp1* Δ*ald2* complemented with pBBR1	This study	19 ± 1	70 ± 5
Δ*rlp1* Δ*ald2*::pBBR1-RpAld2	Δ*rlp1* Δ*ald2* complemented with pBBR1 bearing *ald2*	This study	21 ± 3	17 ± 3
Δ*rlp2* Δ*ald2*	Δ*rlp2* Δ*ald2*	This study	19 ± 4	17 ± 4
Δ*rlp12* Δ*ald2*	Δ*rlp1* Δ*rlp2* Δ*ald2*	This study	21 ± 3	57 ± 4
Δ*rlp12* Δ*ald2*::pBBR1	Δ*rlp12* Δ*ald2* complemented with pBBR1	This study	17 ± 1	65 ± 2
Δ*rlp12* Δ*ald2*::pBBR1-RpAld2	Δ*rlp12* Δ*ald2* complemented with pBBR1 bearing *ald2*	This study	21 ± 1	18 ± 3

[a]*R. palustris* strain CGA009 gene locus identification (ID) numbers from NCBI given in parentheses. St[r], streptomycin resistance.
[b]Doubling times were calculated by least-squares fit of the growth data (during the period in which the growth was in the exponential phase; see Fig. S1 to S6) to the model ln(growth) = $kt + b$ such that doubling time = ln(2)/k. Error bars represent standard errors of the fit data. NG, no growth observed.

for metabolic versatility. Furthermore, we demonstrate *in vivo* and *in vitro* that the *R. palustris* DeepYkr RLP enzyme (RLP1) catalyzes the 5-(methylthio)ribulose-1-P 1,3-isomerization reaction of the MTA-isoprenoid shunt to form 1-(methylthio)xylulose-5-P and 1-(methylthio)ribulose-5-P, whereas the Photo RLP enzyme (RLP2) does not. Finally, under aerobic conditions, both the MTA-isoprenoid shunt and DHAP-methanethiol shunt MSPs appear to be constitutively functional irrespective of the total available sulfur concentration to serve a general housekeeping function in converting MTA to methanethiol. Under anaerobic conditions, the DHAP-methanethiol shunt is inactive. These findings suggest a possible mechanism by which methanethiol, a key component of the global sulfur cycle, is biologically produced by bacteria.

RESULTS

R. palustris contains multiple aerobic methionine salvage pathways linked to methanethiol production. *R. palustris* strain CGA010 is able to grow aerobically on MTA as a sole sulfur source, indicating that it has a functional aerobic MSP for salvaging sulfur from MTA (Table 1) (Fig. S1). However, based on sequence homology, *R. palustris* does not possess any known homologous enzymes of the universal MSP (Fig. 1; black) save for MTA phosphorylase (*mtnP*, RPA4821), 5-(methylthio)ribose-1-P isomerase (*mtnA*, RPA4820), and a putative dioxygenase (*mtnD*, RPA2352). Rather, *R. palustris* encodes the following putative homologues to the *R. rubrum* MTA-isoprenoid shunt genes (Fig. 1; blue) (14, 15): 5-(methylthio)ribulose-1-P 1,3-isomerase (*rlp1*; RPA2169), 1-(methylthio)xylulose-5-P methylsulfurylase (*cupin*; RPA2170), and OAHS sulfhydrylase (*met17*; RPA2362 and RPA4251). In *R. rubrum*, aerobic and anaerobic metabolism of MTA leads to the formation of volatile methanethiol by virtue of the MTA-isoprenoid shunt MSP (Fig. 1; blue) (14, 23). Catalyzed by OAHS sulfhydrylase, methanethiol is coupled to O-acetyl-L-homoserine to regenerate L-methionine (Fig. 1; enzyme N); if not utilized, methanethiol is released into the extracellular environment (14). To determine if a similar MTA-isoprenoid shunt MSP occurred in *R. palustris*, cells were grown aerobically on MTA as the sole sulfur source, washed with sulfur-free media, and then fed [methyl-¹⁴C]MTA. Free thiols generated upon feeding were captured with Ellman's reagent [5,5′-dithiobis-(2-nitrobenzoic acid) (DTNB)] and resolved by reverse-phase
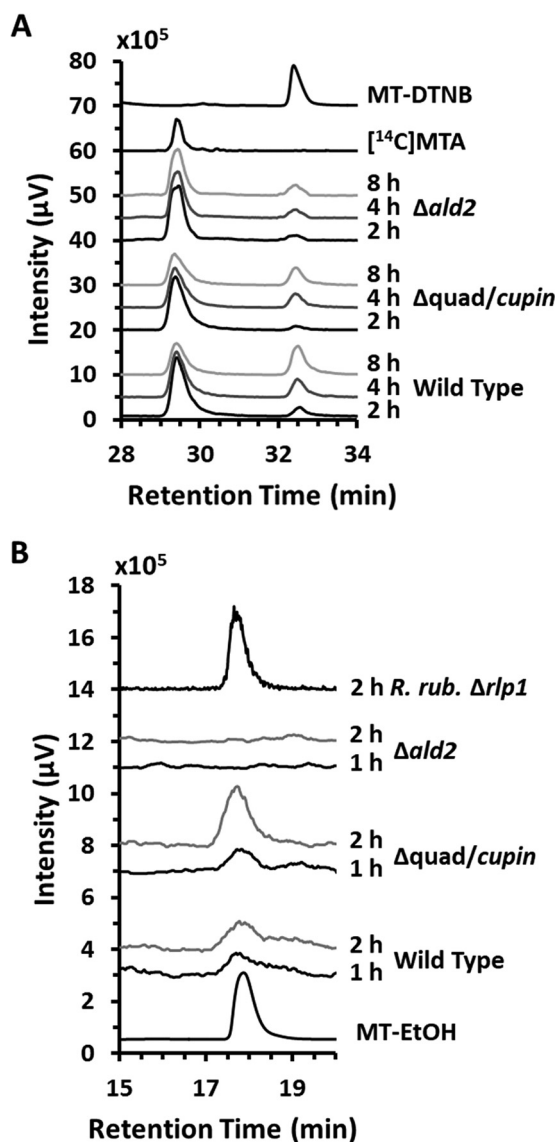
FIG 2 Identification of 2-(methylthio)ethanol and volatile methanethiol produced from [methyl-14C]MTA. (A) Methanethiol and (B) 2-(methylthio)ethanol were identified in various *R. palustris* stains fed aerobically with [methyl-14C]MTA for the indicated amounts of time (h) in the presence of DTNB to capture free thiols released from the cells. Metabolites were separated by reverse-phase HPLC with an in-line radiometric detector. Methanethiol as a DTNB adduct was the only free-thiol species observed. MT-DTNB, unlabeled methanethiol standard as a DTNB adduct detected by 320-nm-wavelength absorbance; [14C]MTA, [methyl-14C]MTA standard. An *R. rubrum* RLP deletion strain (*R. rub. Δrlp1*) was fed anaerobically as a control for 2-(methylthio)ethanol identification since this strain was previously reported to produce 2-(methylthio)ethanol from MTA (15). MT-EtOH, unlabeled 2-(methylthio)ethanol standard detected by 215-nm-wavelength absorbance.

high-performance liquid chromatography (HPLC) with an in-line radiometric detector. As with *R. rubrum* (23), [methyl-14C]methanethiol was observed in *R. palustris* as a DTNB adduct (Fig. 2A), suggesting a functional MTA-isoprenoid shunt in *R. palustris*.

Distinguishing enzymes of the MTA-isoprenoid shunt in *R. rubrum* are the DeepYkr RLP and cupin-type methylsulfurylase (Fig. 1; enzymes L and M) (14). Sequence homology and gene organization suggested that the *R. palustris* DeepYkr RLP (RLP1) (53% identity; E value $9e^{-121}$) and cupin (56% identity; E value $3e^{-50}$) homologues may function like their *R. rubrum* counterparts. Additionally, previous *in vitro* work on functional diversity in the RLP enzyme family indicated that the *R. palustris* Photo RLP (RLP2) may also catalyze an isomerization reaction similar to that seen with the bona

fide *R. rubrum* DeepYkr RLP (22). Therefore, we initially inactivated the DeepYkr RLP (Δ*rlp1*) and Photo RLP (Δ*rlp2*) genes in *R. palustris*. Mutant strains lacking a functional *rlp1* gene or *rlp2* gene or both showed growth similar to that shown by the wild type under aerobic conditions using MTA as the sole sulfur source (Table 1) (Fig. S1).

To determine if methanethiol was still being produced in the absence of a functional RLP in *R. palustris*, cells were grown aerobically on MTA as the sole sulfur source, washed with sulfur-free media, and then fed with MTA. Methanethiol released by the cell upon feeding with MTA was captured with DTNB and measured by reverse-phase chromatography. In the absence of a functional RLP1 (Δ*rlp1* strain or Δ*rlp12* strain), methanethiol was still produced, but at levels that were 4-to-5-fold lower than the wild-type level (Fig. 3A). The level of methanethiol liberated by the *R. palustris* Δ*rlp2* strain was similar to the wild-type level. This indicated that the *R. palustris* DeepYkr RLP (RLP1) and not the Photo RLP (RLP2) was likely involved in the putative MTA-isoprenoid shunt. To further determine the functionality of the putative MTA-isoprenoid shunt, the homologous cupin gene was inactivated in the *R. palustris* wild-type strain (Δ*cupin*). Again, growth on MTA as the sole sulfur source was unaffected (Table 1) (Fig. S1), but the same 4-to-5-fold decrease in the methanethiol level was observed (Fig. 3A). These results indicated that *R. palustris* possesses a putative MTA-isoprenoid shunt in which the DeepYkr RLP and cupin participate. Moreover, since aerobic growth on MTA occurred in the absence of RLP or cupin and since methanethiol was still produced, a separate aerobic MSP must be functional in *R. palustris* that is also linked to methanethiol production. Therefore, we sought to verify the MTA-isoprenoid shunt as well as to characterize this putative additional aerobic MSP in *R. palustris*.

Neither of the RuBisCOs of *R. palustris* contributes to aerobic MTA metabolism. Previous studies of *R. rubrum* revealed that a bona fide RuBisCO is absolutely required to support anaerobic growth on MTA as the sole sulfur source (26). This requirement does not appear to be true simply for cycling the RuBisCO substrate, ribulose-1,5-bisphoshate, because certain mutant RuBisCO enzymes severely compromised in carbon fixation activity are still able to support MTA-dependent growth (23). Rather, it appears that RuBisCO functions specifically in MTA metabolism in *R. rubrum* via an unknown mechanism (26). Recent studies have demonstrated that in both *R. palustris* and *R. rubrum*, RuBisCO not only is synthesized anaerobically but also may be synthesized under aerobic or microaerophilic conditions (27, 28). Indeed, under aerobic growth conditions, deletion of RuBisCO in *R. rubrum* (strain I19* [23]) resulted in a delayed growth phenotype aerobically (Fig. S2) when MTA was used as the sole sulfur source compared to sulfate, suggesting a possible role in aerobic MTA metabolism as well. Therefore, we considered the possibility that one or both of the *R. palustris* RuBisCOs might be functioning in aerobic MTA metabolism. Both the form I RuBisCO gene (*cbbLS*) and the form II RuBisCO gene (*cbbM*), in conjunction with the *cupin* gene, were deleted in the Δ*rlp12* background to form strain Δ*quad* Δ*cupin*. Inactivation of the RuBisCOs had no effect on either aerobic or anaerobic growth using MTA versus sulfate as the sole sulfur source (Table 1) (Fig. S2 and S3). The levels of methanethiol production by *R. palustris* showed negligible differences between the Δ*quad* Δ*cupin* and Δ*rlp12* strains [$t = 3.23$; *P* value $= 0.05$; confidence interval (CI) $= 0.05$] (Fig. 3A), further indicating that RuBisCO was not involved in methanethiol metabolism from MTA. Together, these results support the conclusion that neither of the two RuBisCOs functions in MTA metabolism in *R. palustris*.

MtnP, MtnA, and Ald2 function in the additional *R. palustris* aerobic MSP. Our previous studies of *R. rubrum* and *R. palustris* anaerobic MTA metabolism established the strictly anaerobic DHAP-ethylene shunt MSP (15). Here, MTA phosphorylase (MtnP), 5-(methylthio)ribose-1-P isomerase (MtnA), a class II aldolase-like protein (Ald2) functioning as a 5-(methylthio)ribulose-1P aldolase, and a putative alcohol dehydrogenase (Fig. 1; enzymes D and E and enzymes O and P) sequentially enabled the metabolism of MTA to 2-(methylthio)ethanol and DHAP. Subsequently, but only under anaerobic growth conditions, the 2-(methylthio)ethanol was further metabolized to ethylene and an unknown organo-sulfur intermediate for sulfur salvage (15). Interestingly, *R. palustris*
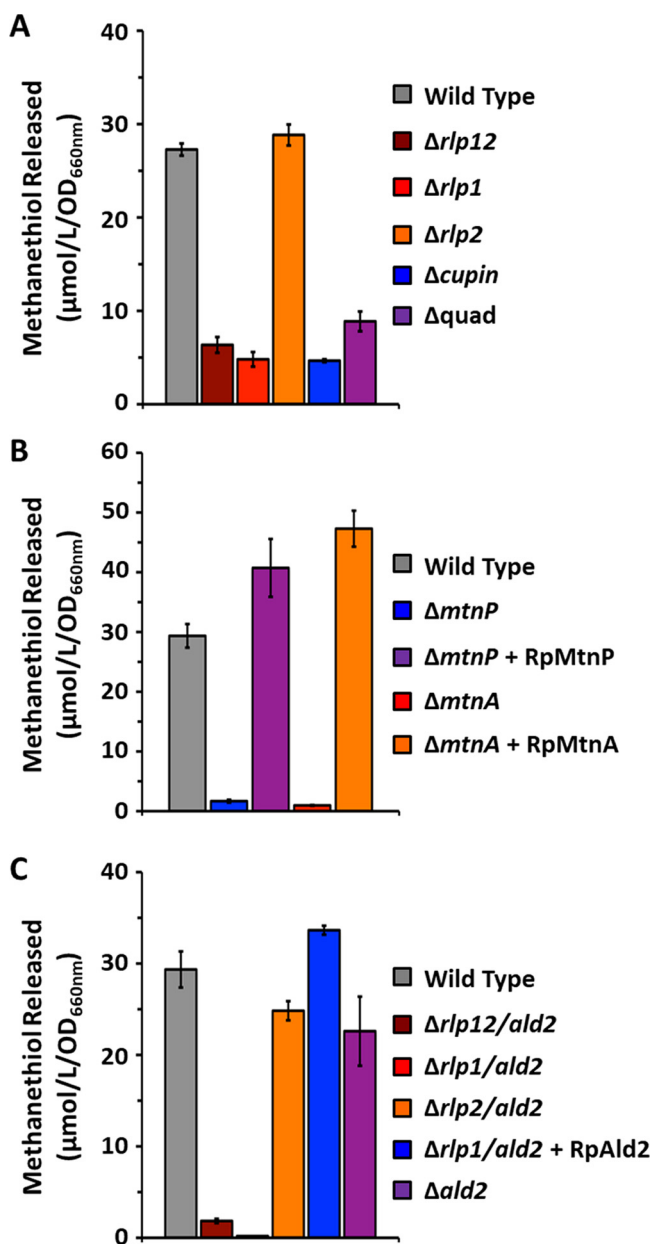
FIG 3 Quantification of volatile methanethiol released by *R. palustris*. (A) Cultures of each indicated strain were initially grown aerobically in the presence of MTA, washed in sulfur-free media containing DTNB, and then fed MTA for 12 h. (B and C) Cultures were initially grown aerobically in the presence of sulfate, washed in sulfur-free media containing DTNB and then fed for 12 h with MTA. The Δ*mtnP* and Δ*mtnA* deletion strains (B) and the Δ*rlp12*, Δ*rlp1*, Δ*rlp2*, and Δ*ald2* deletion strains (C) were complemented with pBBR1-RpMtnP (+ RpMtnP; MTA phosphorylase), pBBR1-RpMtnA [+ RpMtnA; 5-(methylthio)ribose-1-P isomerase], and pBBR1-RpAld2 [+ RpAld2; 5-(methylthio)ribulose-1-P aldolase]. Volatile methanethiol released by the cells was captured as a DTNB adduct and quantified by reverse-phase HPLC based on a standard calibration curve. Data corresponding to the total methanethiol released by the cells during feeding are given in micromoles detected per liter of culture per culture optical density measured at 660 nm (μmol/liter/OD$_{660}$). Error bars indicate standard deviations of results from $n = 3$ independent feeding experiments.

could also grow aerobically on 2-(methylthio)ethanol as a sole sulfur source, suggesting that MtnP, MtnA, and Ald2 may function in this organism in an aerobic MSP involving 2-(methylthio)ethanol that is different from the exclusively anaerobic DHAP-ethylene shunt MSP. Therefore, we systematically quantified the growth of and methanethiol production from *R. palustris* MTA phosphorylase (Δ*mtnP*), 5-(methylthio)ribose-1P isomerase (Δ*mtnA*), and aldolase (Δ*ald2*) gene deletion strains (Table 1).

As observed with *R. rubrum* (14), inactivation of MtnP and MtnA resulted in compromised aerobic growth on MTA as the sole sulfur source (Table 1) (Fig. S4). Furthermore, MTA feeding experiments performed with Δ*mtnP* and Δ*mtnA* deletion strains initially grown on sulfate showed no methanethiol production, in contrast to the wild-type results (Fig. 3B). Upon complementing the Δ*mtnP* and Δ*mtnA* deletion strains with their respective genes expressed in *trans* from a plasmid, both growth (Table 1) (Fig. S4) and methanethiol production (Fig. 3B) were restored to wild-type levels. This demonstrated that MTA phosphorylase (MtnP) and 5-(methylthio)ribose-1-P isomerase (MtnA) are the first two requisite enzymes for both aerobic MSPs, the putative MTA-isoprenoid shunt and the additional pathway, in *R. palustris*.

Next, the putative 2-(methylthio)ribulose-1-P aldolase (*ald2*) gene was inactivated in both the wild-type strain and the Δ*rlp12* deletion strain to construct strains Δ*ald2* and Δ*rlp12* Δ*ald2*, respectively (Table 1). While the aldolase deletion in the wild-type background (Δ*ald2*) was still capable of aerobic growth on MTA as the sole sulfur source, the Δ*rlp12* Δ*ald2* strain exhibited very poor growth (Table 1) (Fig. 4A and S5). Moreover, while the Δ*ald2* deletion strain could still produce methanethiol at ~75% of the wild-type level, negligible methanethiol was observed in the Δ*rlp12* Δ*ald2* deletion strain (Fig. 3C). Complementation of the Δ*rlp12* Δ*ald2* strain with the aldolase expressed in *trans* not only restored growth (Table 1) (Fig. S4A and S5) but also restored methanethiol production to nearly wild-type levels (Fig. 3C). These results confirmed that *R. palustris* has two primary MSPs, a putative MTA-isoprenoid shunt and a second aerobic MSP utilizing Ald2. Again, it was apparent that both pathways required MTA phosphorylase (MtnP) and 5-(methylthio)ribose-1-P isomerase (MtnA) for the initial metabolism of MTA, and both pathways resulted in the generation of volatile methanethiol.

Ald2 links MTA metabolism to 2-(methylthio)ethanol as part of an aerobic methanethiol-producing MSP. We next sought to identify the *in vivo* product(s) of the Ald2-catalyzed reaction of the additional methanethiol-producing MSP. Under anaerobic conditions, in both *R. palustris* and *R. rubrum*, Ald2 functions as a 5-(methylthio)ribulose-1-P aldolase to form DHAP and 2-(methylthio)acetaldehyde as part of the DHAP-ethylene shunt MSP (14, 15). To determine if a similar sequence was occurring aerobically *in vivo*, the wild-type, Δ*quad* Δ*cupin*, and Δ*ald2* strains were fed with [methyl-^{14}C]MTA. Metabolites were extracted and resolved by reverse-phase HPLC with an in-line radiometric detector. As observed for anaerobic MTA metabolism (15), 2-(methylthio)ethanol was produced in the wild-type strain and was undetectable in the aldolase deletion strain (Fig. 2B). In addition, 2-(methylthio)ethanol was enhanced in the Δ*quad* Δ*cupin* strain in which the MTA-isoprenoid shunt was inactivated via knockouts of RLP1 and cupin (*vide infra*). As previously reported (15), observance of 2-(methylthio)ethanol and not 2-(methylthio)acetaldehyde *in vivo* is likely due to rapid conversion of the aldehyde to the less reactive alcohol moiety, presumably by an alcohol dehydrogenase. As such, these results indicate that Ald2 also functions *in vivo* as a 5-(methylthio)ribulose-1-P aldolase to form DHAP and 2-(methylthio)acetaldehyde under aerobic growth conditions in *R. palustris*.

Methanethiol captured by DTNB after feeding the Δ*quad* Δ*cupin* strain with [methyl-^{14}C]MTA was observed as [methyl-^{14}C]methanethiol (Fig. 2A), confirming that the methanethiol produced by the second MSP in which Ald2 participates was also derived from MTA, presumably via 2-(methylthio)ethanol as an intermediate. This was further supported by the observation that *R. palustris* strains fed aerobically with 2-(methylthio)ethanol produced methanethiol at a rate similar to that seen when they were fed with MTA (Table 2). These observations are consistent with the conclusion that *R. palustris* possesses an aerobic DHAP-methanethiol shunt MSP analogous to the anaerobic DHAP-ethylene shunt MSP. There, DHAP and 2-(methylthio)acetaldehyde are produced from MTA by the sequential action of MtnP, MtnA, and Ald2 (14, 15). It is likely an alcohol dehydrogenase catalyzes reduction of 2-(methylthio)acetaldehyde to the observed 2-(methylthio)ethanol, which is further metabolized via some unknown enzyme(s) to produce methanethiol for sulfur salvage (Fig. 6; green).
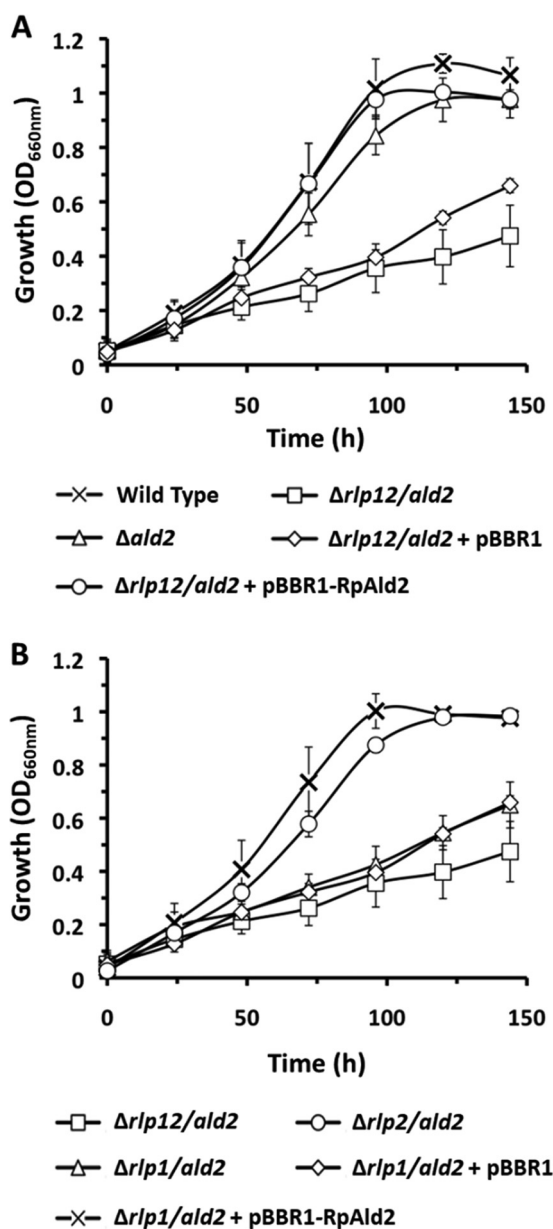
FIG 4 Aerobic growth of *R. palustris* strains by the use of 500 μM MTA as the sole sulfur source. Culture optical density was measured at a 660-nm wavelength (OD$_{660}$). Error bars indicate standard deviations of results from $n = 3$ independent growth experiments. Panels A and B represent the same experiment, but separated into two panels for ease of reading/viewing.

The [methyl-^{14}C]MTA feeding experiments using the wild-type strain versus strains in which the MTA-isoprenoid shunt (strain Δquad Δcupin) or DHAP-methanethiol shunt (strain Δald2) was inactivated enabled measurement of an approximate mass balance in the conversion of MTA to methanethiol for each pathway. Upon feeding each strain, there was a linear decrease in the level of [methyl-^{14}C]MTA due to consumption by the cells and a concomitant linear increase in the level of volatile [methyl-^{14}C]methanethiol released, which was captured and detected as a DNTB adduct. Given that a fraction of the methanethiol formed would have been oxidized or reincorporated into the cell, presumably as methionine and subsequent metabolites, before it could have been captured, the ratio of the rate of methanethiol captured to the rate of MTA consumed gives a lower limit on the mass balance. For the wild-type strain, 62% ± 10% of the MTA consumed was captured as methanethiol on a molar basis. The pathways appeared to

**TABLE 2** Rate of methanethiol release from *R. palustris*

Strain	Growth	$[SO_4^{-2}]$ (μM)	[MTA] (μM)	[MT-EtOH] (μM)	Rate of MT release (μmol/liter/h/OD)[a]
Wild type	Aerobic	0	1,000	0	3.89 $\pm$ 0.19
		0	0	1,000	1.72 $\pm$ 0.56
	Anaerobic	0	1,000	0	3.97 $\pm$ 1.07
		0	0	1,000	n.d.
$\Delta rlp1$	Aerobic	0	1,000	0	0.73 $\pm$ 0.27
		0	0	1,000	1.66 $\pm$ 0.44
	Anaerobic	0	1,000	0	n.d.
		0	0	1,000	n.d.
Wild type	Aerobic	0	0	0	n.d.
		10	0	0	0.01 $\pm$ 0.02
		30	0	0	0.02 $\pm$ 0.01
		100	0	0	0.15 $\pm$ 0.01
		300	0	0	0.15 $\pm$ 0.02
		1,000	0	0	0.14 $\pm$ 0.02
Wild type	Aerobic	10	1,000	0	3.87 $\pm$ 1.19
		100	1,000	0	1.91 $\pm$ 0.37
		1,000	1,000	0	2.56 $\pm$ 0.97

[a]Data represent the rate of methanethiol release from cells in micromoles of methanethiol released per liter of culture per hour per cell culture optical density measured at a 660-nm wavelength (μmol/liter/h/OD). Methanethiol was measured as a DTNB adduct by HPLC based on a standard calibration curve. Error bars indicate standard deviations of results from $n = 3$ independent cultures. n.d., no methanethiol detected.

contribute similarly to this process. For the DHAP-methanethiol shunt (strain $\Delta quad$ $\Delta cupin$), 41% $\pm$ 6% of the MTA consumed was captured as methanethiol, and for the MTA-isoprenoid shunt (strain $\Delta ald2$), it was 32% $\pm$ 4%. Therefore, both the MTA-isoprenoid shunt and the MTA-DHAP shunt appreciably contribute to the aerobic conversion of MTA into methanethiol in *R. palustris*.

Directed metabolite analysis confirms the presence of the MTA-isoprenoid shunt and the role of RLP1 in *R. palustris*. Disruption of the second MSP via inactivation of the *ald2* gene permitted detailed characterization of the putative MTA-isoprenoid shunt, in particular, the possible role of the two RLPs in this pathway. For these studies, [methyl-^{14}C]MTA was fed to the $\Delta ald2$ strain in which both RLPs were active. Free thiols were captured by DTNB and subsequently resolved by HPLC, revealing the production of [methyl-^{14}C]methanethiol (Fig. 2A). This, coupled with the fact that the $\Delta rlp12$ $\Delta ald2$ strain produced negligible amounts of methanethiol, indicated that in the absence of a functional *ald2* gene, the putative MTA-isoprenoid shunt is the likely source for methanethiol. To determine whether RLP1 or RLP2 (or both) functions in this pathway, we separately inactivated each gene in the $\Delta ald2$ background to form strain $\Delta rlp1$ $\Delta ald2$ or strain $\Delta rlp2$ $\Delta ald2$, respectively (Table 1). The $\Delta rlp1$ $\Delta ald2$ strain exhibited the same poor growth phenotype as the $\Delta rlp12$ $\Delta ald2$ strain, whereas the $\Delta rlp2$ $\Delta ald2$ strain grew similarly to the $\Delta ald2$ strain on MTA as the sole sulfur source (Table 1) (Fig. 4B and S6). In addition, upon being fed with MTA, the $\Delta rlp1$ $\Delta ald2$ strain produced negligible amounts of methanethiol, whereas the $\Delta rlp2$ $\Delta ald2$ strain produced methanethiol at levels similar to that produced by the $\Delta ald2$ strain (Fig. 3C). Together with the initial knockout studies in the wild-type background, these results establish that RLP1 functions in MTA metabolism, whereas RLP2 and the two RuBisCOs do not.

In order to identify the specific *in vivo* RLP reaction, strains $\Delta ald2$, $\Delta rlp1$ $\Delta ald2$, and $\Delta rlp2$ $\Delta ald2$ were fed [methyl-^{14}C]MTA. Generated ^{14}C-labeled metabolites were extracted and resolved by the use of a hydrophilic interaction liquid chromatography (HILIC) HPLC instrument equipped with an in-line radiometric detector. Metabolites were identified based on known standards (Fig. 5A). In all 3 strains, 5-(methylthio) ribose-1-P and 5-(methylthio)ribulose-1-P, which are produced by the MTA phosphorylase (MtnP) and 5-(methylthio)ribose-1-P isomerase (MtnA) enzyme reactions, respectively, were identified (Fig. 1; enzymes D and E) (14, 19). Moreover, while
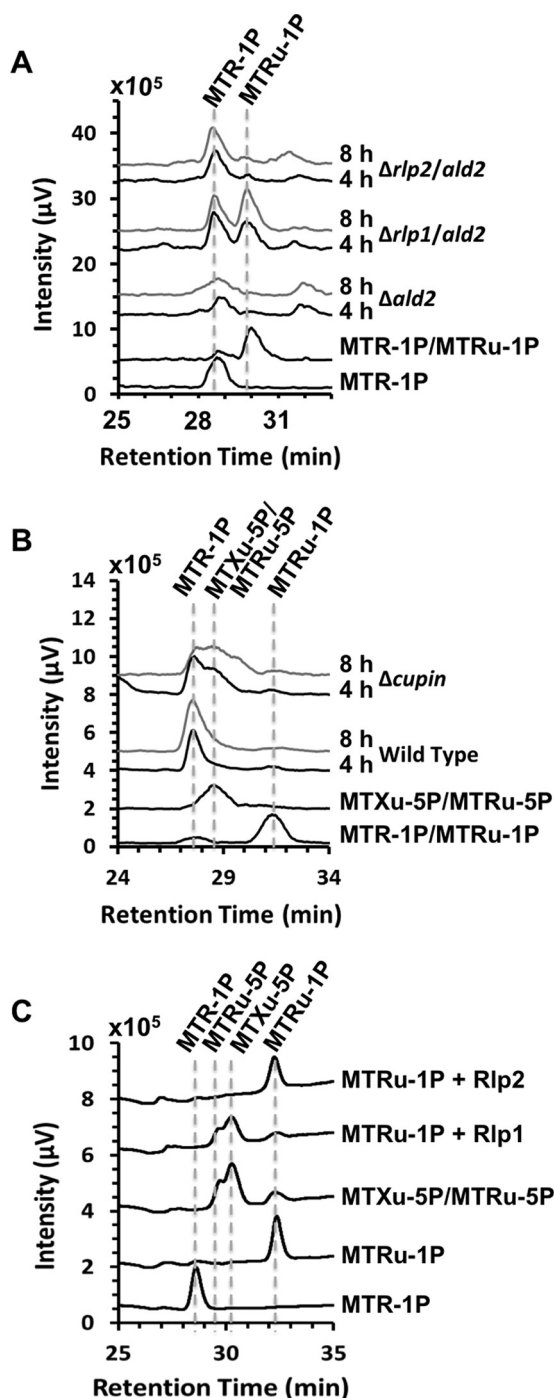
FIG 5 Identification of MTA-isoprenoid shunt MSP intermediates. (A and B) *In vivo* identification of 5-(methylthio)ribose-1-P (MTR-1P), 5-(methylthio)ribulose-1-P (MTRu-1P), and 1-(methylthio)xylulose-5-P (MTXu-5P). Cultures of each indicated strain were initially grown aerobically in the presence of MTA, washed in sulfur-free media, and then fed for the indicated amount of time (indicated in hours) with [methyl-^{14}C]MTA. (A) Metabolites were extracted and ^{14}C-labeled intermediates resolved in by HILIC as reported previously (14) and identified by inline radiometric detector based on known standards. (B) Chromatography conditions were optimized to enhance separation of the species (see Materials and Methods for details). (C) *In vitro* verification of *R. palustris* RLP1 activity corresponding to an MTRu-1P 1,3-isomerase based on known standards. Metabolites were detected by UV absorbance at a 215-nm wavelength (and by use of an in-line radiometric detector; see Fig. S8A).

5-(methylthio)ribulose-1-P was observed at low levels in the Δ*ald2* and Δ*rlp2* Δ*ald2* strains, this compound was observed to have built up in the Δ*rlp1* Δ*ald2* strain (Fig. 5A), further supporting the conclusion that RLP1 functions as the requisite 5-(methylthio)ribulose-1-P 1,3-isomerase in the MTA-isoprenoid shunt.

The inability to observe any specific RLP reaction products in these strains was likely due to the kinetic properties of *R. palustris* MtnA versus successive steps. In *R. rubrum*, the catalytic rate (k_{cat}) of MtnA was low compared to those seen with other enzymes in the pathway. As a result, 5-(methylthio)ribulose-1-P was the dominant species observed and 1-(methylthio)xylulose-5-P was not observable unless the cupin-type methylsulfurylase was inactivated to prevent further metabolism (14). Predicting a similar trend in *R. palustris*, we therefore fed the *R. palustris* wild-type and Δ*cupin* strains with [methyl-^{14}C]MTA (Fig. 5B). In the absence of a functional cupin, 1-(methylthio)xylulose-5-P was observed to build up in the cells. Taken together, these results were consistent with the conclusion that *in vivo* RLP1 but not RLP2 functioned as a 5-(methylthio)ribulose-1-P 1,3-isomerase and that the cupin functioned as a 1-(methylthio)xylulose-5-P methylsulfurylase as part of a functional MTA-isoprenoid shunt (Fig. 6; blue).

As an additional verification that RLP1 and not RLP2 was performing the 5-(methylthio)ribulose-1-P 1,3-isomerization reaction, we recombinantly expressed and purified the *R. rubrum and R. palustris* RLPs by His$_6$-affinity nickel chromatography (see Fig. S7 in the supplemental material). Each RLP was observed as a dimer based on size exclusion chromatography elution times compared to molecular weight standards, consistent with previous reports for the *R. palustris* RLP2 and other RLPs (29). Each RLP was supplied with [methyl-^{14}C]5-(methylthio)ribulose-1-P as a substrate, and products were resolved by HILIC HPLC or reverse-phase HPLC as described above. As in the case of the *R. rubrum* RLP, the *R. palustris* RLP1 also catalyzed the conversion of 5-(methylthio)ribulose-1-P to 1-(methylthio)xylulose-5-P and 1-(methylthio)ribulose-5-P at a 3:1 ratio (Fig. 5C; see also Fig. S8A). In contrast, any products formed from 5-(methylthio)ribulose-1-P by the mediation of RLP2 were below detectable limits and most of the substrate remained unreacted as previously reported (22). Specific formation of 1-(methylthio)xylulose-5-P was further verified by coupled assay with the *R. rubrum* cupin to form methanethiol (Fig. S8B). Subsequent kinetic rate measurement of product formation by the RLP from *R. rubrum* gave a k_{cat} value of 1.2 ± 0.1 s^{-1}; the *R. palustris* RLP1 had a k_{cat} value of 1.3 ± 0.1 s^{-1}, while *R. palustris* RLP2 showed no detectable activity with 5-(methylthio)ribulose-1-P as the substrate. These results confirmed that RLP1 primarily functions as the 5-(methylthio)ribulose-1-P 1,3-isomerase in the *R. palustris* MTA-isoprenoid shunt.

MTA metabolism for volatile methanethiol production appears to be a general housekeeping function. Under sulfur-limiting conditions, various MSPs are observed to be regulated, including the canonical MSP in *Bacillus* sp. (30, 31) and the anaerobic DHAP-ethylene shunt MSP of *R. rubrum* and *R. palustris* (15). For the *R. rubrum* MTA-isoprenoid shunt, previous transcriptomics and proteomics studies showed that enzymes MtnP, MtnA, RLP, and cupin (Fig. 1; enzymes D and E and enzymes L and M) were negligibly regulated whereas the O-acetyl-L-homoserine sulfhydrylase (Fig. 1; enzyme N) was highly upregulated when MTA was used as the sole sulfur source (14, 19, 21). These results were consistent with the observation that cells growing on sulfate that were then fed with MTA produced methanethiol at the same rate as cells grown on MTA and then fed with MTA (14). In other words, the methanethiol-forming sequence appeared to have a general housekeeping function for metabolizing MTA to methanethiol. Then, the O-acetyl-L-homoserine sulfhydrylase was regulated to generate L-methionine when required. However, those previous studies did not address the issue of whether the presence of environmentally available sulfate regulated the formation of methanethiol from MTA.

Given that both *R. palustris* aerobic MSPs led to volatile methanethiol production, we sought to determine if MTA metabolism occurred aerobically in the presence of sulfate by detecting methanethiol release from wild-type cells fed with various com-
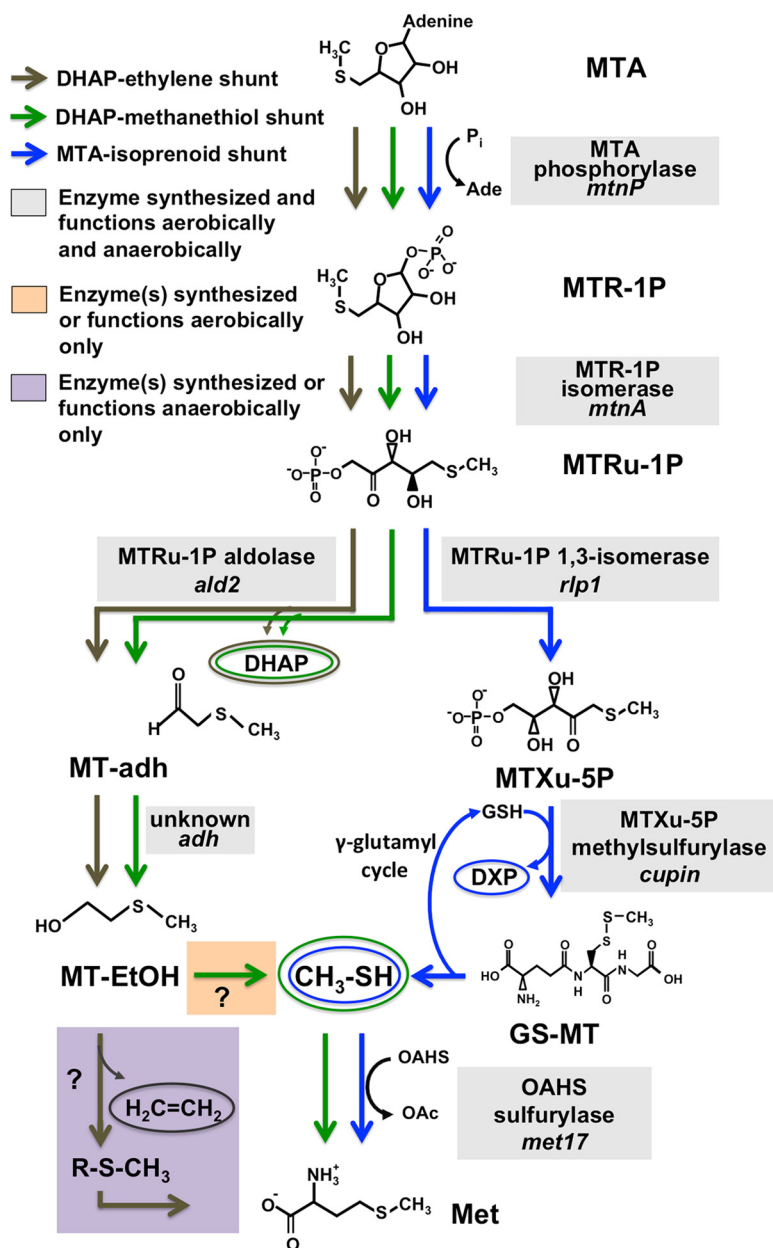
FIG 6 MTA metabolism in *R. palustris*. (Blue) Oxygen-independent MTA-isoprenoid shunt MSP, which functions aerobically (this study) and likely anaerobically (15). (Green) Aerobic DHAP-methanethiol shunt MSP (this study). (Gray) Anaerobic DHAP-ethylene shunt MSP (15). Note that it is likely the same putative unknown alcohol dehydrogenase (*adh*) which functions both aerobically in the MTA-methanethiol shunt and anaerobically in the MTA-ethylene shunt MSPs. However, this step could be catalyzed by different enzymes in the two different scenarios. Compounds were as follows: 5-(methylthio)ribose-1-P (MTR-1P), 5-(methylthio)ribulose-1-P (MTRu-1P), 1-(methylthio)xylulose-5-P (MTXu-5P), 2-(methylthio)acetaldehyde (MT-adh), 2-(methylthio)ethanol (MT-EtOH), 1-deoxyxylulose-5-P (DXP), glutathione (GSH), *S*-methylthio-glutathione (GS-MT), O-acetyl-L-homoserine (OAHS), acetate (OAc). γ-Glutamyl cycle, metabolism of glutathione adducts is initiated by γ-glutamyl transferase, resulting in recovery of glutamate, glycine, and cysteine, which are utilized to regenerate glutathione; the product has been observed to be constitutively expressed in *R. rubrum*, and the pathway is a proposed route for methanethiol release from *S*-methylthio-glutathione (21).

binations of sulfate and MTA. The rate of liberation of methanethiol from fed cells was measured by methanethiol capture with DTNB and detection by reverse-phase HPLC as described above (Table 2). Regardless of the sulfate concentration, volatile methanethiol was generated from the supplied MTA (1 mM) at the same rate. These observa-

tions suggest that, unlike the ethylene-forming step of the anaerobic DHAP-ethylene shunt (15), the presence of sulfate does not regulate aerobic MTA metabolism up through the point of volatile methanethiol release, consistent with a housekeeping function.

To assess methionine salvage and methanethiol formation from the MTA that is produced endogenously by normal cellular processes, cells were incubated with decreasing amounts of sulfate and the rate of methanethiol released by the cells was measured. Methanethiol was released by cells nearly 10-fold faster under sulfate-sufficient conditions (≥100 μM SO_4^{-2}) than under sulfate-limiting conditions (<100 μM SO_4^{-2}) (Table 2). This indicates that under conditions where sulfate is plentiful, a fraction of methanethiol produced from the metabolism of MTA was released into the environment. However, when the total amount of available sulfur became limiting, the vast majority of methanethiol produced by MTA metabolism was further metabolized, presumably by O-acetyl-L-homoserine sulfhydrylase, to generate L-methionine in order to maintain internal sulfur pools.

DISCUSSION

Sulfur availability is imperative for cell viability, underscored by the fact that an estimated 1% to 2% of bacterial dry cell weight is composed of organic sulfur (32). To maintain proper intracellular sulfur pools in low-sulfur environments, many organisms employ salvage pathways for recycling sulfur-containing by-products arising from internal metabolic processes. In many organisms, the dead-end, toxic metabolite 5′-methyl-thioadenosine (MTA) is produced as a result of polyamine, homoserine lactone, ethylene, and betaine lipid biosynthesis. MTA may be subsequently metabolized (or salvaged) back to L-methionine by one of several pathways (Fig. 1). The recent discovery of several new bacterial methionine salvage pathways (MSPs) for the recycling of MTA in oxic and/or anoxic environments reveals that the populations are microbially diverse in salvaging mechanisms. For *R. palustris*, this organism not only possesses an oxygen-independent MTA-isoprenoid shunt (Fig. 6; blue) as evidenced by metabolite identification findings of this study (Fig. 3 and 5) but also utilizes a versatile pathway, linking MTA to 2-(methylthio)ethanol (Fig. 2B) as the key sulfur-containing intermediate in both an aerobic DHAP-methanethiol shunt and anaerobic DHAP-ethylene shunt MSP (Fig. 6; green). In the aerobic DHAP-methanethiol shunt, 2-(methylthio)ethanol is further metabolized to methanethiol, the direct precursor to methionine for sulfur salvage (Table 2) (Fig. 2A). In the anaerobic DHAP-ethylene shunt, 2-(methylthio)ethanol is further metabolized into ethylene and an unknown sulfur-containing intermediate that is presumably further recycled back to methionine (15). Thus, under aerobic conditions *R. palustris* is unique in using two distinct pathways, the MTA-isoprenoid shunt and the DHAP-methanethiol shunt, to metabolize MTA, each resulting in methanethiol production. In contrast, *R. rubrum* uses only the MTA-isoprenoid shunt under aerobic conditions. Under anaerobic conditions, *R. palustris* uses the DHAP-ethylene shunt MSP and likely the MTA-isoprenoid shunt as well (15, 19).

Utilization of a functional MTA-isoprenoid shunt by *R. palustris* signifies that this pathway is not solely specific to *R. rubrum*. At least 25 sequenced bacterial species were observed to possess homologues of the *R. rubrum* RLP and Cupin (>28% and >45% amino acid sequence identity, respectively), as well as putative MTA phosphorylase (MtnP) and 5-(methylthio)ribose-1-P isomerase (MtnA) genes, in a similar organization (14, 19). Of these, 13 are proteobacteria (e.g., *R. rubrum*, *R. palustris* sp., *Rhodomicrobium* sp., and *Nitrosococcus* sp.), while 9 are *Firmicutes* (Dialister sp. and Veillonella sp.) and 2 are *Deinococcus* (Meiothermus sp.).

The discovery here of an aerobic DHAP-methanethiol shunt MSP in which MtnP, MtnA, and 5-(methylthio)ribulose-1-P aldolase (Ald2) participate ascribes a general role for these three enzymes. Together, they catalyze the formation of 2-(methylthio) acetaldehyde from MTA as the key intermediate in at least two distinct methionine salvage pathways. Approximately 6.5% of all sequenced bacteria in the KEGG database possess homologues of these three enzymes, either with their genes all in the same

operon, as in the case of *R. rubrum*, or with *mtnP* and *mtnA* together and *ald2* elsewhere, as in the case of *R. palustris* (15). With regard to habitat, these organisms reside mostly in terrestrial ecosystems; 43% of those species are soil sediment bacteria, as previously noted from a comprehensive genome analysis study analyzing these three key enzymes (15). Besides *R. rubrum* and *R. palustris*, it is unknown whether other organisms possessing MtnP, MtnA, and Ald2 also possess a functional aerobic DHAP-methanethiol shunt and/or anaerobic DHAP-ethylene shunt MSP. Therefore, identification of the methanethiol-catalyzing and ethylene-catalyzing enzymes will be of importance for elucidating the complete pathways.

Role of *R. palustris* RuBisCOs and RuBisCO-like proteins in MTA metabolism. Of all sequenced organisms, *R. palustris* is the only one reported to contain two different subclasses of RLPs as well as two bona fide RuBisCOs. Like its *R. rubrum* counterpart, the DeepYkr RLP (RLP1) of *R. palustris* was found to catalyze the requisite 5-(methylthio) ribulose-1-P 1,3-isomerization step of the MTA-isoprenoid shunt, indicating a potential common functionality for all RLP1-type enzymes, as this is currently the only known *in vivo* function for this subgroup of RLPs. Surprisingly, neither the RuBisCOs nor the Photo RLP (RLP2) appeared to participate by any means in MTA metabolism, either aerobically or anaerobically. Previous *in vitro* characterization of the *R. palustris* RLP2 indicated that it catalyzed a reaction in which only a small percentage of the substrate [5-(methylthio)ribulose-1-P] was converted to 1-(methylthio)xylulose-5-P after extended periods of time (22). It was concluded from this that *R. palustris* RLP2 might also participate in MTA metabolism in this organism. However, in this study, growth phenotypes (Table 1) and *in vivo* metabolite analysis of RLP2 deletion strains (Fig. 3), as well as *in vitro* kinetic rate determinations performed with recombinant enzymes, demonstrated that RLP2 plays a negligible role, if any, in the MTA-isoprenoid shunt and sulfur metabolism in general. Compared to the *C. tepidum* Photo RLP knockout strain (33), the *R. palustris* Photo RLP (RLP2) deletion strain does not present any of the observed pleiotropic effects found in *C. tepidum*, particularly with respect to phototrophic growth on various sulfur sources (25). This further highlights the mechanistic diversity that exists among the various subgroups of RLPs, indicative of their low amino acid sequence homology (25). Further experiments are required to elucidate the specific function of RLP2 in *R. palustris*.

Role of multiple MTA metabolic pathways. *R. palustris* is the first organism to have been observed to possess two aerobic MTA metabolic pathways. Interestingly, the MTA-isoprenoid shunt and DHAP-methanethiol shunt MSPs function simultaneously as evidenced by feeding experiments (Fig. 2B), and both result in the release of methanethiol as an intermediate (Fig. 2A and 3). Why *R. palustris* has two aerobic MSPs that converge to methanethiol and how the fate of 2-(methylthio)ethanol is different under aerobic conditions (DHAP-methanethiol shunt) from that under anaerobic conditions (DHAP-ethylene shunt) are unclear. That *R. rubrum* cannot metabolize 2-(methylthio) ethanol aerobically but can do so anaerobically (15) suggests that a different set of enzymes catalyzes the remaining unknown terminal steps of the DHAP-methanethiol and DHAP-ethylene shunt MSPs. Regardless, given that the MTA-isoprenoid shunt channels five carbon units of the MTA backbone into isoprenoid synthesis via DXP and that the DHAP-methanethiol and DHAP-ethylene shunt MSPs channel three carbon units of the MTA backbone into central carbon metabolism via DHAP, these pathways are poised to help *R. palustris* and similar organisms balance carbon pools in situations in which the MTA metabolism rate is elevated (e.g., polyamine synthesis, quorum sensing, betaine lipid metabolism, sulfate limitation [8, 10, 30]). Presumably, most of the DHAP generated during aerobic MTA metabolism enters into glycolysis for conversion into D-glyceraldehyde 3-phosphate, whereas the DHAP is likely used for ribulose-1,5-bisphosphate regeneration as part of the Calvin-Benson-Bassham cycle under anaerobic conditions.

MTA-isoprenoid shunt and DHAP-methanethiol shunt as housekeeping pathways for metabolism of MTA to methanethiol. Previous experiments performed with

both *R. palustris* and *R. rubrum* indicated that ethylene production via the anaerobic DHAP-ethylene shunt was downregulated by the presence of excess sulfate (15). In contrast, neither the MTA-isoprenoid shunt nor the aerobic DHAP-methanethiol shunt appeared to be upregulated through the generation of methanethiol by the presence of saturating levels ($\geq$100 μM) of sulfate (Table 2). This is consistent with earlier observations of *R. rubrum* (14) and observations here of *R. palustris* indicating that, regardless of the sulfur source used to grow cultures (MTA or sulfate), volatile methanethiol was liberated from the cells into the environment at the same rates upon feeding with MTA. In addition, the *R. rubrum mtnP*, *mtnA*, *rlp1*, *cupin*, and *ald2* genes all do not appear to be appreciably regulated by the presence of MTA under either aerobic or anaerobic conditions (19, 21). Altogether, these findings are consistent with a housekeeping role for these pathways with respect to the metabolism of MTA to methanethiol under aerobic conditions.

When the total available level of sulfur became limiting (<100 μM), the rate of methanethiol release by the cells decreased (Table 2). Under such conditions, sulfur is a valuable commodity and is presumably conserved to maintain cellular sulfur pools by metabolizing all available methanethiol into methionine via O-acetyl-L-homoserine sulfhydrylase. In *R. rubrum*, expression of the O-acetyl-L-homoserine sulfhydrylase genes (*R. rubrum* A0774 [Rru_A0774] and Rru_A0784) is upregulated over 10-fold in the presence of MTA (14, 19). *R. palustris* has four O-acetyl-L-homoserine sulfhydrylase homologues (RPA2350, RPA2364, RPA4251, and RPA4766), so this organism presumably may also use one or more of these enzymes to recycle methanethiol to methionine. In addition, under conditions where available sulfur is plentiful, excess methanethiol produced by MTA metabolism that is not required by the cell may be liberated into the environment as volatile methanethiol.

Methanethiol and dimethyl sulfide (DMS) are two of the most important volatile organic sulfur compounds in terms of the global sulfur cycle (34), and DMS is a contributing factor in numerous environmental functions, including global warming, acid precipitation, and cloud formation (35, 36). An average of 38 to 40 Tg of DMS is released into the atmosphere annually, making it the most abundant organic sulfur gas emitted globally (34). In marine surface waters, bacteria utilize dimethylsulfoniopropionate (DMSP), produced by unicellular algae as an osmolyte, resulting in the production of DMS and methanethiol by-products (37). DMSP demethylation pathways result in the production of methanethiol, which can be further utilized to form methionine or released into the environment. Cleavage of DMSP by DMSP lyase directly results in the formation of DMS. Some studies suggest that when cells have sufficient sulfur pools, DMSP degradation switches from demethylation to cleavage (38). While DMSP metabolism is the major marine source of methanethiol and DMS, it is increasingly evident that alternate routes may significantly contribute to their production by terrestrial ecosystems. Many bacteria, particularly those from soil ecosystems (up to 76%), possess a methanethiol-dependent DMS synthase (MddA), which transfers the methyl group from SAM to methanethiol to form DMS (39). Other thio-methyltransferase reactions in bacteria, catalyzing the methylation of hydrogen sulfide to methanethiol and methanethiol to DMS, have also been reported (34, 39). However, their distribution and role in environmental methanethiol and DMS production are not as well understood. Typically, it has been assumed or observed that methanethiol is produced either by a thiol-methyltransferase (34) or by the degradation of methionine via methionine gamma lyase (39, 40). The results of the current study reveal that the previously unidentified MTA-isoprenoid shunt and/or the MTA-DHAP shunt pathways may also contribute to the production of volatile methanethiol in the environment. It is likely that *R. palustris* and other organisms further utilize methanethiol produced by these pathways, either as a sulfur source or for the production of DMS. Indeed, *R. palustris* encodes a homologue of methanethiol *S*-methyltransferase (RPA2835), which catalyzes the conversion of methanethiol into dimethyl sulfide via transmethylation from SAM (39). It will be of interest to determine the contribution of these newly discovered

methanethiol-generating pathways to the total levels of methanethiol and DMS in the environment as well as to denote the bacteria that employ these pathways.

MATERIALS AND METHODS

Bacterial strains and growth conditions. *R. palustris* strains used in the current study are listed in Table 1 and were derived from wild-type strain CGA010. The *R. rubrum* wild-type strain (ATCC 11170), a RLP deletion strain (Δ*rlp*, strain "WR"), and a form II RuBisCO (*cbbM*) deletion strain with a *nifA* (M173V) mutation (Δ*cbbM* Δ*nifA*$_{M173V}$; strain I19*) are described elsewhere (26, 41). *E. coli* strain SM10 (Biomedal Lifescience) was used for plasmid transfer via conjugative mating into *R. palustris*. *E. coli* strains BL21(DE3) (Millipore) with a pG-TF2 chaperone plasmid (TaKaRa) and Rosetta2(DE3) pLysS (Millipore) were used for recombinant protein synthesis.

All *E. coli* strains were grown aerobically in lysogeny broth (LB) media at 37°C with shaking at 280 rpm unless otherwise noted. All *R. palustris* strains were initially grown aerobically in PYE complex medium (0.3% peptone, 0.3% yeast extract, 10% Ormerod's basal salts [42], 1 mg/liter thiamine, 1 mg/liter nicotinic acid, 15 μg/liter biotin) supplemented with 50 μg/liter streptomycin at 30°C with shaking at 280 rpm.

For growth studies, *R. palustris* cultures initially grown in PYE complex medium were washed aerobically three times in sulfur-free Ormerod's malate minimal media (OMM) (26) containing 20 mM DL-malate, 1 mg/liter thiamine, 1 mg/liter nicotinic acid, 15 μg/liter biotin, and 15 μM 4-aminobenozic acid. Washed cells were used to inoculate 10 ml of OMM in either a capped 22-by-175-mm culture tube (aerobic growth studies) or a 20-by-145-mm sealed anaerobic culture tube (anaerobic growth studies) to an initial optical density at 660 nm (OD$_{660}$) of ~0.03. Cultures were then supplemented with 500 μM ammonium sulfate or 500 μM MTA and incubated at 30°C either aerobically in the dark with shaking at 280 rpm or anaerobically in an incandescent lighted chamber (1,500 lx). *R. rubrum* growth studies were performed as previously reported (26).

Generation of *R. palustris* deletion strains and complementation vectors. In-frame nonpolar gene deletions were created by double homologous recombination using the pK18mobsacB suicide vector and sucrose selection, as previously reported (15, 43). Plasmids for deletion of *R. palustris rlp1*, *rlp2*, *ald2*, and *cupin* were as previously reported (15). For deletion of *R. palustris* RuBisCO form I (*cbbLS*) and form II (*cbbM*) genes, mutant strains were obtained as previously reported (44). Fragments were digested with appropriate restriction enzymes (New England Biolabs) and ligated into digested suicide vector pK18mobsacBst (15). The resulting plasmids were transformed into *E. coli* SM10 and transferred to *R. palustris* by conjugative mating. Transconjugants and double recombinants harboring the desired deletions were screened as previously described (15, 43). Antibiotics for transconjugant selection were kanamycin (50 μg/ml) and streptomycin (500 μg/ml).

Gene complementation of *R. palustris* deletion strains was performed via plasmid-based gene expression from the LacZ promoter using pBBR1-MCS5 (see Table S1 in the supplemental material). Plasmids pBBR1-RpMtnP (where "RpMtnP" represents "*R. palustris* MtnP"), pBBR1-RpMtnA, and pBBR1-RpAld2 were as previously reported (15) for gene expression of *R. palustris mtnP*, *mtnA*, and *ald2*, respectively. Conjugative transfer of plasmids via biparental mating between *E. coli* SM10 and *R. palustris* was performed as previously described (15). Transconjugants were selected using streptomycin (500 μg ml^{-1}).

Identification of [methyl-^{14}C]MTA-derived metabolites. All [methyl-^{14}C]-labeled standards were synthesized from [methyl-^{14}C]S-adenosyl-L-methionine (PerkinElmer) as previously reported (19). *R. palustris* strains were grown aerobically in 50 ml of sulfur-free OMM supplemented with 200 μM MTA to an OD$_{660}$ of ~0.4. Cells were washed twice with sulfur-free OMM and resuspended to a final OD$_{660}$ of ~8.0 to 10.0 in 2.5 ml of sulfur-free OMM as previously reported (14). Cells were fed with 20 μM MTA and 30 μM [methyl-^{14}C]MTA. Cell suspensions were placed in 5-ml conical glass vials and bubbled with compressed filtered air while being shaken at 60 rpm in a 30°C water bath. For detection of methanethiol, 500 μM DTNB was also added to the media. Time point data were acquired by pelleting a 300-μl cell suspension, separating cells from the media by centrifugation, and storing at −80°C.

For detection of [methyl-^{14}C]-labeled 2-(methylthio)ethanol and methanethiol-DTNB adduct, metabolites present in the media were separated by Zorbax C$_{18}$ reverse-phase chromatography (Agilent) at 30°C with a flow rate of 0.8 ml/min on a Shimadzu Prominence HPLC system with an inline UV light-visible light (UV-Vis) detector (215 nm, 260 nm, and 320 nm) and a β-RAM radiometric detector (IN/US Systems). Metabolites were eluted on a gradient composed of buffer A with 0.2% buffer B for 5 min, 0.2% to 50% buffer B for 23 min, 50% to 100% buffer B for 14 min, and 100% buffer B for 3 min, followed by reequilibration with 0.2% buffer B for 12 min (buffer A, 20mM ammonium acetate; buffer B, 20 mM ammonium acetate and 50% acetonitrile; pH to 6.8 using acetic acid).

For detection of [methyl-^{14}C]-labeled (methylthio)pentose-phosphate sugars, cell supernatants were concentrated by vacuum centrifugation to 100 μl and 400 μl of acetonitrile was added. Cell pellets were subsequently extracted twice with 250 μl of this mixture by subjecting cells to vortex mixing for 5 min at room temperature (RT) followed by incubation at −20°C for 15 min and centrifugation to remove cell debris. Initially, extracted metabolites were separated as previously described (14) by HILIC-HPLC on a SeQuant ZIC-pHILIC column (Millipore) using UV-Vis detection (215 nm and 260 nm) and an inline radiometric detector (Fig. 5) as described above. Separation of metabolites was optimized using a modified gradient as follows: 100% buffer B for 5 min, 100% to 40% buffer B for 40 min, and 40% to 100% buffer B for 10 min, followed by reequilibration with 100% buffer B for 15 min. Coordinately, the flow rates were 0.35 ml/min for 15 min, 0.35 to 0.25 ml/min

for 2 min, 0.25 ml/min for 28 min, and 0.25 to 0.35 ml/min for 2 min, followed by 0.35 ml/min for 23 min (buffer A, 20 mM ammonium bicarbonate; buffer B, 20 mM ammonium bicarbonate and 80% acetonitrile; pH 9.2 using ammonium hydroxide).

Methanethiol release measurements. *R. palustris* strains were grown aerobically in 50 ml of sulfur-free OMM supplemented with 500 μM MTA or 500 μM sulfate to an OD_{660} of 0.3 to 0.5. Cells were washed twice with sulfur-free OMM and resuspended to a final OD_{660} of 3.0 to 5.0 in 5 ml sulfur-free OMM as previously reported (14). Cells were fed with 1 mM MTA, and Ellman's reagent [5,5′-dithiobis-(2-nitrobenzoic acid) (DTNB)] was added to reach 500 μM. Cells were incubated at 30°C with shaking at 280 rpm for 15 h, after which 250 μl of cell suspension was centrifuged to collect the media. Released methanethiol, captured as a DTNB adduct (MT-DTNB), was separated by reverse-phase HPLC as described above. MT-DTNB was detected at 360-nm-wavelength absorbance and quantified based on an MT-DTNB standard calibration curve.

Gene expression and purification of recombinant proteins. Plasmids for expression of the *Bacillus subtilis mtnK* and *mtnA* genes and of the *R. rubrum rlp1* and *ald2* genes were as previously reported (14). Expression plasmids for *R. palustris rlp1* and *rlp2* genes and *E. coli* DXP reductoisomerase (*DRI*) genes (Table S1) were created by amplifying each gene via PCR using primers with restriction enzyme sites in Table S2 and cloning into pET28 (Millipore). *B. subtilis mtnK* and *mtnA, R. rubrum rlp,* and *E. coli dri* were expressed for 3 h in strain Rosetta2(DE3) pLysS grown in LB media at 37°C with shaking at 280 rpm supplemented with kanamycin (50 μg/ml), chloramphenicol (34 μg/ml), and 1 mM IPTG (isopropyl-β-D-thiogalactopyranoside). Proteins were purified as previously described (44). To increase protein solubility, *E. coli* BL21(DE3) pG-TF2 was used for expression of *rlp1* and *rlp2*. Cells were initially grown at 37°C with shaking at 280 rpm to an OD_{660} of ~0.5 in LB media supplemented with kanamycin, chloramphenicol, and tetracycline (2 μg/ml). Cells were cold shocked on ice for 30 min and supplemented with 125 μM IPTG, and expression proceeded for 12 h at 15°C with shaking at 180 rpm. Due to high coexpression of chaperone proteins, RLP1 and RLP2 were purified by a linear gradient (10 column volumes) of 20 to 250 mM imidazole in 300 mM NaCl–50 mM Tris-Cl (pH 7.5) on a 10-ml column of nickel-nitrilotriacetic acid (Ni-NTA) agarose (Qiagen). Purified proteins were buffer exchanged into a mixture of 20 mM Tris-Cl (pH 7.5), 1 mM EDTA (pH 8.0), 1 mM dithiothreitol (DTT), and 300 mM NaCl by the use of a centrifugal concentrator (Amicon, Millipore). Size exclusion chromatography was performed at 4°C using a Superose 12 column (GE Life Science) equilibrated with the buffer described above at 0.5 ml/min. Glycerol was added to reach a level of 10%, and proteins were stored at −80°C. Protein concentrations were determined by UV absorbance, and purity was assessed by SDS-PAGE (Fig. S7).

Enzyme assays. The activity and kinetics of the RLP enzymes were determined by a coupled spectrophotometric assay following the oxidation of NAPDH at a 340-nm wavelength using a spectrophotometer (Carey, Varian). 5-(Methylthio)ribulose-1-P was produced *in situ* using 0.5 mM 5-(methylthio)ribose, 1 mM ATP, 2.5 mM $MgCl_2$, 10 μM *B. subtilis* MtnK, and 10 μM MtnA. *R. rubrum* or *R. palustris* RLP was added to 0 to 300 nM, and production of 1-(methylthio)xylulose-5-P was monitored by adding 10 μM *R. rubrum* Cupin, 10 μM *E. coli* DRI, 1 mM DTT, 1 mM $MnCl_2$, and 0.4 mM NADPH.

Identification of specific products of the RLP enzymes with 5-(methylthio)ribulose-1-P as the substrate was accomplished by HILIC. 5-(Methylthio) ribose (1 μM) and [methyl-^{14}C]5-(methylthio)ribose (50 μM) were added to a reaction mixture containing 10 mM $MgCl_2$, 50 mM HEPES (pH 7.5), 5 mM ATP, 2 mM DTT, 20 μM *B. subtilis* MtnK, 10 μM *B. subtilis* MtnA, and 10 μM RLP in a 50-μl total volume. Reaction mixtures were incubated at 30°C for 2 h, acetonitrile was added to reach a 300-μl total volume, and then the reaction mixture was separated by HILIC-HPLC with UV detection at a 215-nm wavelength and in-line radiometric detection as described above. Specific production of 1-(methylthio)xylulose-5-P was further confirmed by adding to the reaction mixtures described above 2 mM DTT, 1 mM $MnCl_2$, and 10 μM *R. rubrum* cupin. Reactions were stopped by addition of 10 mM DTNB, and [methyl-^{14}C]methanethiol as a DTNB adduct was resolved by reverse-phase HPLC with UV detection at a 320-nm wavelength and in-line radiometric detection as described above.

SUPPLEMENTAL MATERIAL

Supplemental material for this article may be found at https://doi.org/10.1128/mBio .00407-18.

FIG S1, TIF file, 0.1 MB.
FIG S2, TIF file, 0.1 MB.
FIG S3, TIF file, 0.2 MB.
FIG S4, TIF file, 0.1 MB.
FIG S5, TIF file, 0.1 MB.
FIG S6, TIF file, 0.1 MB.
FIG S7, TIF file, 0.6 MB.
FIG S8, TIF file, 0.3 MB.
TABLE S1, DOCX file, 0.1 MB.
TABLE S2, DOCX file, 0.1 MB.

REFERENCES

1. Wetzel RG. 2001. Iron, sulfur, and silica cycles, p 310–322. In Limnology: lake and river ecosystems. Academic Press, Cambridge, MA.

2. Wang F, Tessier A, Buffle J. 1998. Voltammetric determination of elemental sulfur in pore waters. Limnol Oceanogr 43:1353–1361. https://doi.org/10.4319/lo.1998.43.6.1353.

3. Steinmann P, Shotyk W. 1997. Chemical composition, pH, and redox state of sulfur and iron in complete vertical porewater profiles from two sphagnum peat bogs, Jura Mountains, Switzerland. Geochim Cosmochim Acta 61:1143–1163. https://doi.org/10.1016/S0016-7037(96)00401-2.

4. Zhou W, He P, Li S, Lin B. 2005. Mineralization of organic sulfur in paddy soils under flooded conditions and its availability to plants. Geoderma 125:85–93. https://doi.org/10.1016/j.geoderma.2004.07.005.

5. Wind T, Conrad R. 1995. Sulfur compounds, potential turnover of sulfate and thiosulfate, and numbers of sulfate-reducing bacteria in planted and unplanted paddy soil. FEMS Microbiol Ecol 18:257–266. https://doi.org/10.1111/j.1574-6941.1995.tb00182.x.

6. Parveen N, Cornell KA. 2011. Methylthioadenosine/S-adenosylhomocysteine nucleosidase, a critical enzyme for bacterial metabolism. Mol Microbiol 79:7–20. https://doi.org/10.1111/j.1365-2958.2010.07455.x.

7. Sauter M, Moffatt B, Saechao MC, Hell R, Wirtz M. 2013. Methionine salvage and S-adenosylmethionine: essential links between sulfur, ethylene and polyamine biosynthesis. Biochem J 451:145–154. https://doi.org/10.1042/BJ20121744.

8. Schaefer AL, Greenberg EP, Oliver CM, Oda Y, Huang JJ, Bittan-Banin G, Peres CM, Schmidt S, Juhaszova K, Sufrin JR, Harwood CS. 2008. A new class of homoserine lactone quorum-sensing signals. Nature 454:595–599. https://doi.org/10.1038/nature07088.

9. Ma JF, Shinada T, Matsuda C, Nomoto K. 1995. Biosynthesis of phytosiderophores, mugineic acids, associated with methionine cycling. J Biol Chem 270:16549–16554. https://doi.org/10.1074/jbc.270.28.16549.

10. Tamot B, Benning C. 2009. Membrane lipid biosynthesis in purple bacteria, p 595–599. *In* Hunter CN, Daldal F, Thurnauer MC, Beatty JT (ed), The purple phototrophic bacteria. Advances in photosynthesis and respiration, vol 28. Springer, Dordrecht, the Netherlands. https://doi.org/10.1007/978-1-4020-8815-5_7.

11. Sun J, Daniel R, Wagner-Döbler I, Zeng AP. 2004. Is autoinducer-2 a universal signal for interspecies communication: a comparative genomic and phylogenetic analysis of the synthesis and signal transduction pathways. BMC Evol Biol 4:36. https://doi.org/10.1186/1471-2148-4-36.

12. Schroeder HR, Barnes CJ, Bohinski RC, Mallette MF. 1973. Biological production of 5-methylthioribose. Can J Microbiol 19:1347–1354. https://doi.org/10.1139/m73-217.

13. Albers E. 2009. Metabolic characteristics and importance of the universal methionine salvage pathway recycling methionine from 5′-methylthioadenosine. IUBMB Life 61:1132–1142. https://doi.org/10.1002/iub.278.

14. Erb TJ, Evans BS, Cho K, Warlick BP, Sriram J, Wood BM, Imker HJ, Sweedler JV, Tabita FR, Gerlt JA. 2012. A RuBisCO-like protein links SAM metabolism with isoprenoid biosynthesis. Nat Chem Biol 8:926–932. https://doi.org/10.1038/nchembio.1087.

15. North JA, Miller AR, Wildenthal JA, Young SJ, Tabita FR. 2017. Microbial pathway for anaerobic 5′-methylthioadenosine metabolism coupled to ethylene formation. Proc Natl Acad Sci U S A 114:E10455–E10464. https://doi.org/10.1073/pnas.1711625114.

16. Sekowska A, Danchin A. 2002. The methionine salvage pathway in *Bacillus subtilis*. BMC Microbiol 2:8. https://doi.org/10.1186/1471-2180-2-8.

17. Sekowska A, Dénervaud V, Ashida H, Michoud K, Haas D, Yokota A, Danchin A. 2004. Bacterial variations on the methionine salvage pathway. BMC Microbiol 4:9. https://doi.org/10.1186/1471-2180-4-9.

18. Nakano T, Ohki I, Yokota A, Ashida H. 2013. MtnBD is a multifunctional fusion enzyme in the methionine salvage pathway of *Tetrahymena thermophila*. PLoS One 8:e67385. https://doi.org/10.1371/journal.pone.0067385.

19. North JA, Sriram J, Chourey K, Ecker CD, Sharma R, Wildenthal JA, Hettich RL, Tabita FR. 2016. Metabolic regulation as a consequence of anaerobic 5-methylthioadenosine recycling in *Rhodospirillum rubrum*. MBio 7:e00855-16. https://doi.org/10.1128/mBio.00855-16.

20. Warlick BP, Evans BS, Erb TJ, Ramagopal UA, Sriram J, Imker HJ, Sauder JM, Bonanno JB, Burley SK, Tabita FR, Almo SC, Sweedler JS, Gerlt JA. 2012. 1-Methylthio-D-xylulose 5-phosphate methylsulfurylase: a novel route to 1-deoxy-D-xylulose 5-phosphate in *Rhodospirillum rubrum*. Biochemistry 51:8324–8326. https://doi.org/10.1021/bi301215g.

21. Cho K, Evans BS, Wood BM, Kumar R, Erb TJ, Warlick BP, Gerlt JA, Sweedler JV. 2014. Integration of untargeted metabolomics with transcriptomics reveals active metabolic pathways. Metabolomics https://doi.org/10.1007/s11306-014-0713-3

22. Warlick BP. 2013. Rhodospirillum rubrum/deep Ykr RLP family. Functional discovery and promiscuity in the RuBisCO superfamily. PhD dissertation. University of Illinois at Urbana-Champaign, Champaign, IL. http://hdl.handle.net/2142/45444.

23. Dey S, North JA, Sriram J, Evans BS, Tabita FR. 2015. In vivo studies in *Rhodospirillum rubrum* indicate that ribulose-1,5-bisphosphate carboxylase/oxygenase (RuBisCO) catalyzes two obligatorily required and physiologically significant reactions for distinct carbon and sulfur metabolic pathways. J Biol Chem 290:30658–30668. https://doi.org/10.1074/jbc.M115.691295.

24. Larimer FW, Chain P, Hauser L, Lamerdin J, Malfatti S, Do L, Land ML, Pelletier DA, Beatty JT, Lang AS, Tabita FR, Gibson JL, Hanson TE, Bobst C, Torres JL, Peres C, Harrison FH, Gibson J, Harwood CS. 2004. Complete genome sequence of the metabolically versatile photosynthetic bacterium *Rhodopseudomonas palustris*. Nat Biotechnol 22:55–61. https://doi.org/10.1038/nbt923.

25. Hanson TE, Tabita FR. 2003. Insights into the stress response and sulfur metabolism revealed by proteome analysis of a *Chlorobium tepidum* mutant lacking the RuBisCO-like protein. Photosynth Res 78:231–248. https://doi.org/10.1023/B:PRES.0000006829.41444.3d.

26. Singh J, Tabita FR. 2010. Roles of RuBisCO and the RuBisCO-like protein in 5-methylthioadenosine metabolism in the nonsulfur purple bacterium *Rhodospirillum rubrum*. J Bacteriol 192:1324–1331. https://doi.org/10.1128/JB.01442-09.

27. Narancic T, Scollica E, Kenny ST, Gibbons H, Carr E, Brennan L, Cagney G, Wynne K, Murphy C, Raberg M, Heinrich D, Steinbüchel A, O'Connor KE. 2016. Understanding the physiological roles of polyhydroxybutyrate (PHB) in *Rhodospirillum rubrum* S1 under aerobic chemoheterotrophic conditions. Appl Microbiol Biotechnol 100:8901–8912. https://doi.org/10.1007/s00253-016-7711-5.

28. Rey FE, Harwood CS. 2010. FixK, a global regulator of microaerobic growth, controls photosynthesis in *Rhodopseudomonal palustris*. Mol Microbiol 75:1007–1020. https://doi.org/10.1111/j.1365-2958.2009.07037.x.

29. Tabita FR, Hanson TE, Li H, Satagopan S, Singh J, Chan S. 2007. Function, structure, and evolution of the RuBisCO-like proteins and their RuBisCO homologs. Microbiol Mol Biol Rev 71:576–599. https://doi.org/10.1128/MMBR.00015-07.

30. Coppée JY, Auger S, Turlin E, Sekowska A, Le Caer JP, Labas V, Vagner V, Danchin A, Martin-Verstraete I. 2001. Sulfur-limitation-regulated proteins in *Bacillus subtilis*: a two-dimensional gel electrophoresis study. Microbiology 147:1631–1640. https://doi.org/10.1099/00221287-147-6-1631.

31. Mansilla MC, Albanesi D, de Mendoza D. 2000. Transcriptional control of the sulfur-regulated *cysH* operon, containing genes involved in L-cysteine biosynthesis in *Bacillus subtilis*. J Bacteriol 182:5885–5892. https://doi.org/10.1128/JB.182.20.5885-5892.2000.

32. Fagerbakke KM, Heldal M, Norland S. 1996. Content of carbon, nitrogen, oxygen, sulfur, and phosphorous in native aquatic and cultured bacteria. Aquat Microb Ecol 10:15–27. https://doi.org/10.3354/ame010015.

33. Hanson TE, Tabita FR. 2001. A ribulose-1,5-bisphosphate carboxylase/oxygenase (RuBisCO)-like protein from *Chlorobium tepidum* that is involved with sulfur metabolism and the response to oxidative stress. Proc Natl Acad Sci U S A 98:4397–4402. https://doi.org/10.1073/pnas.081610398.

34. Bentley R, Chasteen TG. 2004. Environmental VOSCs-formation and degradation of dimethyl sulfide, methanethiol and related materials. Chemosphere 55:291–317. https://doi.org/10.1016/j.chemosphere.2003.12.017.

35. Bates TS, Charlson RJ, Gammon RH. 1987. Evidence for the climatic role of marine biogenic sulphur. Nature 329:319–321. https://doi.org/10.1038/329319a0.

36. Berresheim H, Eisele FL, Tanner DJ, McInnes LM, Ramsey-Bell DC, Covert DS. 1993. Atmospheric sulfur chemistry and cloud condensation nuclei (CCN) concentrations over the northeastern Pacific Coast. J Geophys Res 98:12701–12711. https://doi.org/10.1029/93JD00815.

37. Yoch DC. 2002. Dimethylsulfoniopropionate: its sources, role in the marine food web, and biological degradation to dimethyl sulfide. Appl Environ Microbiol 68:5804–5815. https://doi.org/10.1128/AEM.68.12.5804-5815.2002.

38. Kiene RP, Linn LJ, González J, Moran MA, Bruton JA. 1999. Dimethylsulfoniopropionate and methanethiol are important precursors of methionine and protein-sulfur in marine bacterioplankton. Appl Environ Microbiol 65:4549–4558.

39. Carrión O, Curson AR, Kumaresan D, Fu Y, Lang AS, Mercadé E, Todd JD. 2015. A novel pathway producing dimethylsulphide in bacteria is widespread in soil environments. Nat Commun 6:6579. https://doi.org/10.1038/ncomms7579.

40. Sato D, Nozaki T. 2009. Methionine gamma-lyase: the unique reaction mechanism, physiological roles, and therapeutic applications against infectious diseases and cancers. IUBMB Life 61:1019–1028. https://doi.org/10.1002/iub.255.

41. Wang D, Zhang Y, Welch E, Li J, Roberts GP. 2010. Elimination of RuBisCO alters the regulation of nitrogenase activity and increases hydrogen production in *Rhodospirillum rubrum*. Int J Hydr Energy 35:7377–7385. https://doi.org/10.1016/j.ijhydene.2010.04.183.

42. Ormerod JG, Ormerod KS, Gest H. 1961. Light-dependent utilization of organic compounds and photoproduction of molecular hydrogen by photosynthetic bacteria; relationships with nitrogen metabolism. Arch Biochem Biophys 94:449–463. https://doi.org/10.1016/0003-9861(61)90073-X.

43. Romagnoli S, Tabita FR. 2006. A novel three-protein two-component system provides a regulatory twist on an established circuit to modulate expression of the *cbbI* region of *Rhodopseudomonas palustris* CGA010. J Bacteriol 188:2780–2791. https://doi.org/10.1128/JB.188.8.2780-2791.2006.

44. Satagopan S, Chan S, Perry LJ, Tabita FR. 2014. Structure-function studies with the unique hexameric form II ribulose-1,5-bisphosphate carboxylase/oxygenase (RuBisCO) from *Rhodopseudomonas palustris*. J Biol Chem 289:21433–21450. https://doi.org/10.1074/jbc.M114.578625.